Korean J. of Chem. Eng., 12(5), 540-550 (1995)

PULSATILE FLOWS IN STENOSED BLOOD VESSELS

Youngsul Jeong and In Seok Kang†

Department of Chemical Engineering and Advanced Fluids Engineering Research Center,
Pohang University of Science and Technology, San 31 Hyoja Dong, Pohang 790-784, Republic of Korea
(Received 8 March 1995 • accepted 6 July 1995)

Abstract—The pulsatile blood flows in solid blood vessels are investigated numerically in order to understand some physiological phenomena in arteries. For the geometry of the blood vessels, one-point stenosed and periodically stenosed blood vessels are considered. Taking advantage of axisymmetry in the problem, the stream function-vorticity formulation is used for the governing equations of the fluid flows. All the computations are performed by using the ADI scheme of the finite difference method on the numerically generated boundary-fitted orthogonal curvilinear coordinate systems. The flow fields are found to be dramatically different depending on the Strouhal number. When the Strouhal number is O(1) or larger, the flow field is quite dynamic in the sense that the vortices formed during the previous period survive and exert residual stress on the blood vessel wall. On the other hand, when the Strouhal number is as small as $O(10^{-2})$, the flow fields are found to be in the quasi-steady state. The computation results suggest that the deterioration of endothelial cells may occur due to strong local flow fields near the stenosis and that the probability of platelet attachment to the blood vessel wall is higher in the region behind the stenosis. From the results for the periodically stenosed vessel, the so-called steady streaming phenomenon is confirmed. The steady streaming effect in a wavy channel is expected to increase the heat and mass transfer rate without making the flow turbulent.

Key words: Pulsatile Flows, Stenosed Blood Vessel, Numerical Solution

INTRODUCTION

The fluid mechanical study of blood flow in artery bears some important aspects due to the engineering interests as well as the feasible medical applications. In China, the concept of blood circulation was stated very clearly in one of the oldest books on medicine, the Nei Jing, or "Internal Classic." With this knowledge, Chinese could diagnose diseases by taking pulses at a wrist where the radial artery passes close to the surface. Chinese already knew empirically that the abnormal waves are associated with diseases. However, the rational explanations about the diagnostic method have been lacked.

The clinical diagnoses of diseases by measuring the abnormal blood pressure waves have been practiced from ancient times without reasonable explanations. However, in view of the recent advancement of fluid mechanics, it would be wonderful if the "empirical practice" could be transformed to the "scientific medicine." One possible scenario is to record the pulse patterns by using the instruments along with the analyses based on the advanced mathematical modelling. By comparing the results of physiological experiments with the theoretical predictions, the pulse patterns may be correlated with the types of diseases in a rational way. Although the transformation to the scientific medicine cannot be achieved in the near future, this general direction sheds a light on the possible contribution of fluid mechanists to the medicine area.

Because many cardiovascular disorders are closely associated with the flow conditions in the blood vessel, the characteristics of blood flow in arteries have received much attention. The flow patterns in an arterial segment, or in a model of the segment, have mainly been determined experimentally. Another approach to the problem of calculating flow characteristics in blood vessels is possible by using numerical methods. The computer simulation of blood flows in the models of vessel segments yields good results and provides useful information on the flow patterns. The objective of this work is also to understand the physical events that take place in the aortic blood vessel by using the numerical methods and thereby to contribute to improvement of the physiological understanding.

Previous works on the blood flows in arteries can be roughly classified into two categories: one is for the arterial section without bifurcation and the other for the section near the branching point. Several important issues are well explained in reference books [Pedley, 1980; Patel and Vaishnav, 1980; Fung, 1984]. The present work belongs to the former category. The analyses for the arterial section without bifurcation aim mainly at better understanding of the flow field change due to the stenosis developed on the aterial wall and/or the pressure wave pattern due to the blood flow in an elastic blood vessel. Daly [1976] analyzed the pulsatile flow through stenosed canine femoral arteries by using the numerical scheme of the Arbitrary Lagrangian Eulerian (ALE) procedure. His results suggested that the time averaged peak wall shear may be sufficiently large, when the areal restriction is 61%, to result in the development of atheromatous lesions and endothelial damage proximal to the stenosis. A similar problem of pulsatile flow in a constricted 2-d channel was studied by Tutty [1992]. Due to the physiological significance, the pressure wave pattern in an elastic blood vessel has been studied by many researchers [Womesley, 1955; Ling and Atabek, 1972; Wu et al., 1984; Dutta et al., 1992; Ma et al., 1992]. One of the prominent works

†To whom all correspondences should be addressed.

in this area was done by Ling and Atabek [1972]. They took account of the nonlinear terms of the Navier-Stokes equations as well as the nonlinear behavior of the arterial wall. Recently, the research trend in this field has directed toward the numerical analysis of the flow of a Newtonian fluid in an elastic tube when the fluid is subjected to an oscillatory pressure gradient [Wu et al., 1984; Dutta et al., 1992; Ma et al., 1992]. However, the effect of stenosis on the pressure wave pattern has not been considered yet.

One commonly encountered phenomenon in studying the pulsatile flow in a solid or an elastic wavy vessel is the so-called steady streaming effect. Briefly speaking, the steady streaming effect refers to a kind of flow (usually circulating vortex) existing inside the vessel until the inertial force of the imposed flow exceeds the power of the vortex. Wang and Tarbell [1992] studied the steady streaming effect inside the elastic tube and discussed the possible applications to physiological flows. Kaneko and Honji [1979] studied the steady streaming induced by oscillatory viscous flow of small amplitude over a fixed wavy wall. However, the most thorough analysis on the steady streaming effect was done by Sobey [1980, 1983]. He presented numerical solutions of the time-dependent two dimensional Navier-Stokes equation inside the physical domain of furrowed channel with a detailed explanation on the mechanism. On application side, those researches have mainly aimed at the development of biomedical engineering equipments owing to the merit in improving the heat or mass transfer by using the non-turbulent unsteady flows.

The purpose of this study is to simulate the physiological phenomena that occur in the stenosed aorta and femoral arteries which are 0.5-2 cm of diameter without bifurcation. As a first step to achieve the goal, we consider the solid blood vessel case for simplicity and take two types of physical models in this work. One is the one-point deep stenosed blood vessel which is in the normal state in the remaining part, and the other is a periodically stenosed wavy vessel.

At this initial stage, the present work is quite similar to the previous works [Daly, 1976; Sobey 1980]. There are, however, several new aspects in addition to the detailed geometrical differences. The first major difference is in the numerical scheme. The boundary-fitted-orthogonal grid systems are used in our study while the non-orthogonal grid systems have been adopted in the previous works. Owing to the advantages in simplicity and convergence, our analysis on the fixed blood vessel problem can be easily extended to the moving elastic vessel problem. The other point is that a much wider range of the Strouhal number, which is the ratio of the unsteady acceleration to the steady acceleration, is considered in this work to see the effect of unsteadiness of the flow.

In the following section, we briefly summarize the characteristics of the blood flows in artery before starting the analysis.

BLOOD FLOWS IN ARTERY

With each contraction the left ventricle ejects a volume of blood into the aorta and thence on into the arterial bed. A pressure wave moves rapidly through the arterial system where it can be felt as the arterial pulse. Blood pressure in the arterial system varies with the cardiac cycle, reaching a systolic peak and a diastolic trough, the levels of which are measured by sphygmomanometer. The difference between systolic and diastolic pressures is known as the pulse pressure.

As mentioned earlier, analysis of the pulsatile blood flows is important in engineering applications as well as in medical applications. But the exact solution to this problem has not been available so far. This is mainly due to the complex physiological situations in the artery. The reason why the problem is so complicated may well be understood by examining the real situations of blood flow in arteries.

· First, the blood is a non-Newtonian fluid. The constitutive equation of blood is more complicated compared with that of the Newtonian fluid. As a result, highly nonlinear form is produced in the final equations for the blood flow.

· Second, the blood vessel is an elastic tube rather than a static fixed pipe. The wall of the blood vessel, which is the boundary of the domain where the problem is stated, fluctuates as time goes on. In mathematics, the moving boundary problems are much more difficult to be treated compared with the fixed boundary problems.

· Third, the blood flow is pulsatile. Thus the oscillatory behavior of the blood flow in an elastic arterial vessel must be considered.

· Fourth, the blood flow in the vessel is a combination of turbulent and laminar flows. In medium- and small-sized vessels the flow is laminar, but in a comparatively large-sized vessel, turbulent flow is observed in some cases.

· Fifth, the straight segments are short in human arterial system. So only the developing flows exist.

· Sixth, the arterial system has almost infinitely many branches and there exist bi-, tri-, and multi-furcations in the blood vessel.

If we considered all of these in one setting of the mathematical modelling, the final system of equations would be highly nonlinear and extremely coupled. The problem may be too difficult to be solved even with the most high-powered computers. Thus, in this paper, we simplify the situation as much as possible to make the problem tractable without losing the essence.

METHOD OF ANALYSIS

1. Equations of Motion of the Blood Flow

The physical models and the coordinate systems are shown in Fig. 1. As mentioned in Introduction, only the cases of static fixed blood vessels are considered in this paper. The equations which govern the axisymmetric pulsatile flow are the continuity and the Navier-Stokes equations. The followings are assumed to simplify the governing equations:

· The blood is a homogeneous incompressible Newtonian fluid.

· The density and the viscosity of the fluid are constant.

· The flow is laminar.

The following characteristic scales are adopted to non-dimensionalize the governing equations

$$u_c=\bar{u}_{max},\ t_c=\frac{1}{\Omega},\ p_c=\rho u_c^2,\ l_c=R,\ \text{and}\ \nabla_c=\frac{1}{l_c}$$

where, $\bar{u}_{max}$ is the time-averaged velocity at the center of the entrance plane of the vessel, R the radius of the vessel at the entrance point, and Ω the oscillatory frequency of the imposed pulsatile flow times 2π. Then the dimensionless governing equations become

$$\nabla\cdot\mathbf{u}=0, \tag{1}$$

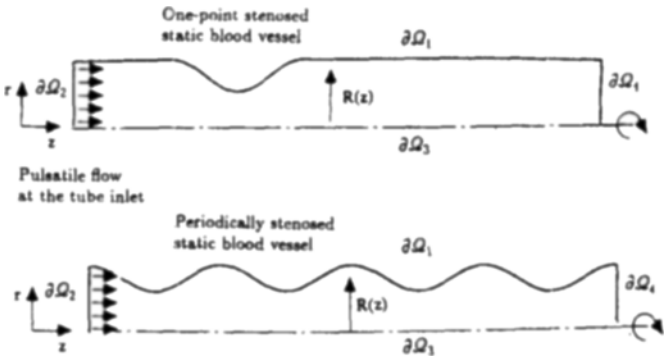

Fig. 1. Physical models and coordinate systems considered in this study.

$$St\frac{\partial \mathbf{u}}{\partial t}+\mathbf{u}\cdot\nabla\mathbf{u}=-\nabla p+\frac{1}{Re}\nabla^2\mathbf{u}. \tag{2}$$

In (2), two important dimensionless numbers appear. The Strouhal number, $St=\Omega l_c/u_c$, is the ratio of unsteady acceleration to the steady acceleration and is the measure of the unsteadiness of the flow. The Reynolds number, $Re=u_c l_c/\nu$, is the ratio of the inertial force to the viscous force. In some literatures, these two dimensionless parameters are combined to form the pulsatile Reynolds number, $\alpha^2=ReSt(=l_c^2\Omega/\nu)$, which stands for the degree of oscillation of the flow inside the blood vessel. In arteries, the value of the Reynolds number ranges from $O(10^2)$ to $O(10^3)$ and that of the Strouhal number from $O(10^{-2})$ to $O(10^{-1})$. In the present study, the values of Re=100, 250, and St=0.01, 0.5, 1.0 are used.

2. Stream Function-Vorticity Formulation

In this work we adopt the stream function-vorticity formulation by taking advantage of axisymmetry in the problem. The vorticity equation is

$$St\frac{\partial \omega}{\partial t}-\nabla\times(\mathbf{u}\times\omega)=\frac{1}{Re}\nabla^2\omega \tag{3}$$

where ω is the vorticity vector defined by

$$\omega=\nabla\times\mathbf{u}. \tag{4}$$

Since we deal with the axisymmetric blood flows without swirling in arteries, only the $\mathbf{e}_3$-directional vorticity component remains, i.e.

$$\omega=\omega_3\mathbf{e}_3.$$

Now, we have to transform Eqs. (3) and (4) into the form appropriate to the axisymmetric general orthogonal coordinate system. In an orthogonal $\xi-\eta-\phi$-coordinate system, the differential displacement vector is represented as

$$\begin{aligned}d\mathbf{x}&=h_1d\xi_1\mathbf{e}_1+h_2d\xi_2\mathbf{e}_2+h_3d\xi_3\mathbf{e}_3\\&=h_\xi d\xi\mathbf{e}_\xi+h_\eta d\eta\mathbf{e}_\eta+h_\phi d\phi\mathbf{e}_\phi\end{aligned}$$

where h_ξ, h_η, and h_ϕ are the scale factors in the directions of ξ, η, and ϕ, respectively. In axisymmetric problems, $h_\phi=r$ holds, and we define the stream function as

$$u_\xi=-\frac{1}{h_\eta h_\phi}\frac{\partial\Psi}{\partial\eta},\quad u_\eta=\frac{1}{h_\xi h_\phi}\frac{\partial\Psi}{\partial\xi},$$

to satisfy the continuity equation automatically. Since only the vorticity component ω_3 remains, we set $\omega=\omega_3$. Then the governing equations for the vorticity ω and the stream function Ψ are obtained from Eq. (3) and the definition of the vorticity equation [Eq. (4)]. The resulting equations are

$$\begin{aligned}&St\frac{\partial\omega}{\partial t}+\frac{h_\phi}{h_\xi}u_\xi\frac{\partial}{\partial\xi}\left(\frac{\omega}{h_\phi}\right)+\frac{h_\phi}{h_\eta}u_\eta\frac{\partial}{\partial\eta}\left(\frac{\omega}{h_\phi}\right)\\&=\frac{1}{Reh_\xi h_\eta}\left\{\frac{\partial}{\partial\xi}\left[\frac{f}{h_\phi}\frac{\partial(h_\phi\omega)}{\partial\xi}\right]+\frac{\partial}{\partial\eta}\left[\frac{1}{fh_\phi}\frac{\partial(h_\phi\omega)}{\partial\eta}\right]\right\}\end{aligned} \tag{5}$$

$$\frac{1}{h_\xi h_\eta}\left[\frac{\partial}{\partial\xi}\left(\frac{f}{h_\phi}\frac{\partial\Psi}{\partial\xi}\right)+\frac{\partial}{\partial\eta}\left(\frac{1}{fh_\phi}\frac{\partial\Psi}{\partial\eta}\right)\right]=\omega \tag{6}$$

where f is the distortion function defined by $f=h_\eta/h_\xi$ (see Batchelor [1967]).

The above equations are rearranged into the following form

$$q_0\frac{\partial W}{\partial t}=f^2\frac{\partial^2W}{\partial\xi^2}+\frac{\partial^2W}{\partial\eta^2}+q_1\frac{\partial W}{\partial\xi}+q_2\frac{\partial W}{\partial\eta}+q_3W+q_4, \tag{7}$$

where W represents ω or Ψ. The appropriate coefficients q_0, q_1, q_2, q_3, q_4 are written in Table 1. We use the ADI (Alternating Direction Implicit) method to obtain the numerical solution of the above governing equations. To solve the equations by ADI method, we use the central difference approximation for the spatial derivatives. We then obtain the difference equations for the vorticity

$$q_0^n\frac{\omega^*-\omega^n}{1/2\Delta t}=f^2\frac{\delta^2\omega^*}{\delta\xi^2}+\frac{\delta^2\omega^n}{\delta\eta^2}+q_1^n\frac{\delta\omega^*}{\delta\xi}+q_2^n\frac{\delta\omega^n}{\delta\eta}+q_3^n\omega^*+q_4^n \tag{8}$$

$$\begin{aligned}q_0^n\frac{\omega^{n+1}-\omega^*}{1/2\Delta t}=&f^2\frac{\delta^2\omega^*}{\delta\xi^2}+\frac{\delta^2\omega^{n+1}}{\delta\eta^2}+q_1^n\frac{\delta\omega^*}{\delta\xi}+q_2^n\frac{\delta\omega^{n+1}}{\delta\eta}\\&+q_3^n\omega^{n+1}+q_4^n\end{aligned} \tag{9}$$

where Δt is the time step used in ADI scheme.

The same scheme does not work for the stream function equation because q_0 is zero. In other words, the stream function equation does not have the time derivative term. Therefore the stream function equation should be satisfied at any time and the discretized version of stream function equation

Table 1. Coefficients of the governing equations

$$q_0\frac{\partial W}{\partial t}=f^2\frac{\partial^2W}{\partial\xi^2}+\frac{\partial^2W}{\partial\eta^2}+q_1\frac{\partial W}{\partial\xi}+q_2\frac{\partial W}{\partial\eta}+q_3W+q_4$$

W	q
ω	$q_0: h_\eta^2 Re\,St$
	$q_1: -Reu_\xi h_\eta f+f\frac{\partial f}{\partial\xi}+\frac{f^2}{h_\phi}\frac{\partial h_\phi}{\partial\xi}$
	$q_2: -Reu_\eta h_\xi f-\frac{1}{f}\frac{\partial f}{\partial\eta}+\frac{1}{h_\phi}\frac{\partial h_\phi}{\partial\eta}$
	$q_3: \frac{Reu_\xi h_\eta f}{h_\phi}\frac{\partial h_\phi}{\partial\xi}+\frac{Reu_\eta h_\xi f}{h_\phi}\frac{\partial h_\phi}{\partial\eta}-\left(\frac{f}{h_\phi}\frac{\partial h_\phi}{\partial\xi}\right)^2-\left(\frac{1}{h_\phi}\frac{\partial h_\phi}{\partial\eta}\right)^2$
	$q_4: 0$
Ψ	$q_0: 0$
	$q_1: f\frac{\partial f}{\partial\xi}-\frac{f^2}{h_\phi}\frac{\partial h_\phi}{\partial\xi}$
	$q_2: -\frac{1}{f}\frac{\partial f}{\partial\eta}-\frac{1}{h_\phi}\frac{\partial h_\phi}{\partial h}$
	$q_3: 0$
	$q_4: -\omega h_\eta^2 h_\phi$

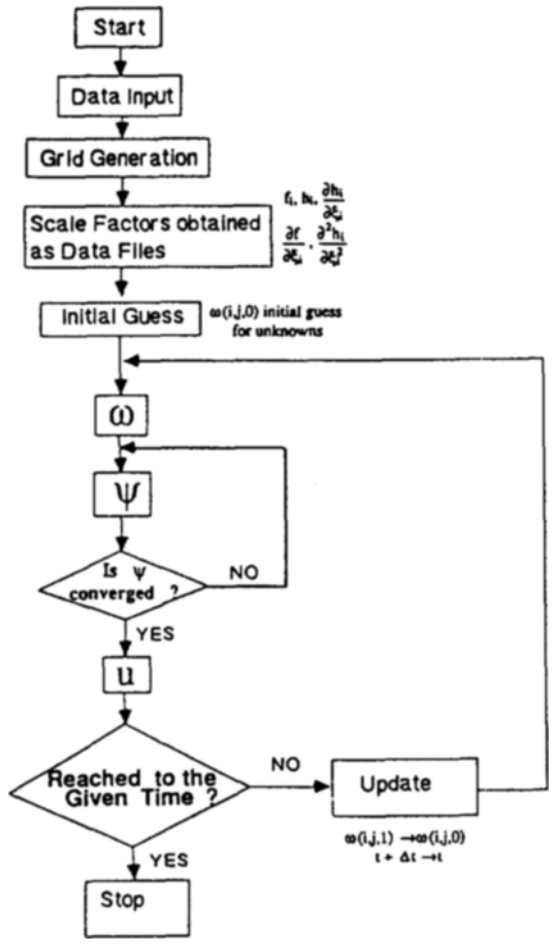

Fig. 2. Flow diagram for the numerical scheme.

$$f^2\frac{\delta^2\Psi^n}{\delta\xi^2}+\frac{\delta^2\Psi^n}{\delta\eta^2}+q_1\frac{\delta\Psi^n}{\delta\xi}+q_2\frac{\delta\Psi^n}{\delta\eta}+q_3\Psi^n+q_3{}^n=0 \tag{10}$$

should be satisfied for all $t=n\Delta t$ $(n=0,1,2,3,\cdots)$. As we can see in Table 1, $q_4=-\omega h_\eta{}^2 h_\phi$ for the stream function equation. Thus, for each time-step, we should solve (10) for the given $q_4{}^n=-\omega^n h_\eta{}^2 h_\phi$, which is obtained from the n-th time-step value of the vorticity. Eq. (10) can be solved in various ways. But an easy way is to transform (10) into the fictitious time-dependent problem and adopt ADI method to obtain the converged solution

$$\frac{\Psi^{\nu+1/2}-\Psi^\nu}{1/2\tau}=f^2\frac{\delta^2\Psi^{\nu+1/2}}{\delta\xi^2}+\frac{\delta^2\Psi^\nu}{\delta\eta^2}+q_1\frac{\delta\Psi^{\nu+1/2}}{\delta\xi}+q_2\frac{\delta\Psi^\nu}{\delta\eta}+q_3\Psi^{\nu+1/2}+q_4{}^n \tag{11}$$

$$\frac{\Psi^{\nu+1}-\Psi^{\nu+1/2}}{1/2\tau}=f^2\frac{\delta^2\Psi^{\nu+1/2}}{\delta\xi^2}+\frac{\delta^2\Psi^{\nu+1}}{\delta\eta^2}+q_1\frac{\delta\Psi^{\nu+1/2}}{\delta\xi}+q_2\frac{\delta\Psi^{\nu+1}}{\delta\eta}+q_3\Psi^{\nu+1/2}+q_4{}^n \tag{12}$$

where ν is the iteration number. In (11) and (12), the fictitious time-step size τ plays a role of iteration parameter and is of O (10^{-2}) in the present study. In the present work, the convergence criterion for the stream function equation is

$$\max|\Psi_{ij}^{\nu+1/2}-\Psi_{ij}^{\nu}|,\ \max|\Psi_{ij}^{\nu+1}-\Psi_{ij}^{\nu+1/2}|<10^{-9}.$$

Thus, the maximum residual of (10) is $O(10^{-7})$.

The overall solution algorithm is presented in Fig. 2. As we can see in the figure, for each time step increase, i.e. from $t=t$ to $t=t+\Delta t$, ω^{n+1} is simply obtained by (8) and (9) for the given ω^n. Once ω^{n+1} is obtained, the stream function equation is solved iteratively until the fully converged solution Ψ^{n+1} corresponding to ω^{n+1} is obtained.

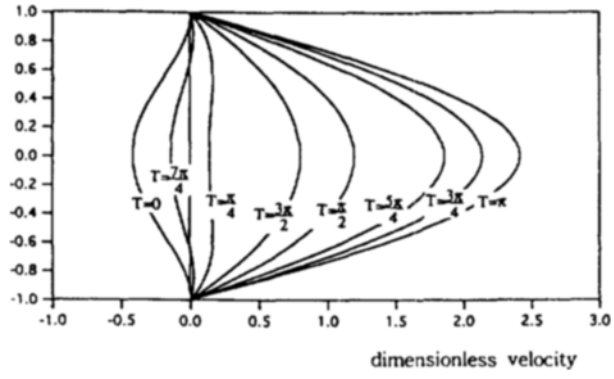

Fig. 3. The velocity profiles of the flow imposed at the tube inlet (results of Eq. (13); reference [19]).

For the boundary conditions, we have considered the following facts. At the solid surface ($\partial\Omega_1$), no slip condition holds. At the inlet ($\partial\Omega_2$), the pulsatile velocity profile is imposed. The unsteady pulsatile velocity profile imposed at the vessel inlet is given in the next subsection. The symmetry condition at the center line ($\partial\Omega_3$) is due to the axisymmetry of the flow in the channel. For the outlet ($\partial\Omega_4$), we have assumed $\partial/\partial z=0$ for the one-point stenosed tube, and that all variables at the outlet plane are the same as those at the plane one-period ahead of the end point for the periodically wavy blood vessel.

3. Pulsatile Flow at the Vessel Inlet

In the present work, we want to investigate the effects of St and Re on the flow fields in the one-point stenosed and the periodically stenosed blood vessels when a specific pulsatile flow is imposed at the inlet. For the pulsatile flow specified at the inlet, we have used the velocity components given by

$$u_z=\left[(1+\varepsilon\sin t)(1-r^2)-\varepsilon\frac{\alpha^2}{4}\left(\frac{3}{4}-r^2+\frac{r^4}{4}\right)\cos t\right];\ u_r=0 \tag{13}$$

with $\alpha^2=37.75$ and $\varepsilon=0.2$ in all computations. The pulsatile velocity profiles predicted by (13) with the parameter values are shown in Fig. 3. Although the expression is simple, the resulting velocity profiles have some essential features of the pulsatile blood flow in arteries. Particularly, the back flow for a short time interval is noteworthy.

Here, a comment should be given to the velocity field in (13). Originally, the expression in (13) was obtained as an asymptotic form of the solution of the problem of uni-directional flow in a circular tube with constant radius produced by the time-periodic pressure gradient

$$-\frac{\partial p}{\partial z}=G_0(1+\varepsilon\sin t). \tag{14}$$

The solution to the problem is given by a complicated expression including the Bessel functions. The asymptotic form of the solution for the case of $\alpha^2=\mathrm{ReSt}\ll 1$ is in fact given in dimensionless form as (see Leal [19])

$$u_z=\left[(1+\varepsilon\sin t)(1-r^2)-\varepsilon\frac{\alpha^2}{4}\left(\frac{3}{4}-r^2+\frac{r^4}{4}\right)\cos t+O(\alpha^4)\right]. \tag{15}$$

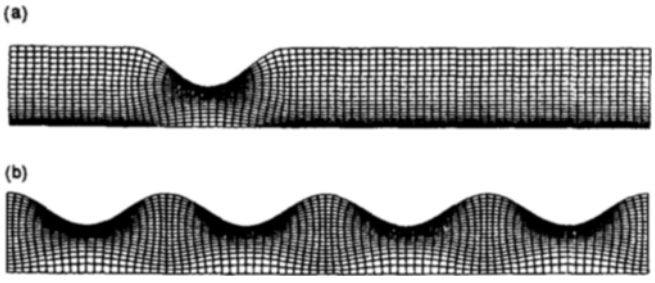

Fig. 4. Orthogonal grid systems inside the blood vessels.
(a) one-point stenosed blood vessel type
(b) periodically stenosed blood vessel type

The typical value of α^2 was found to be 37.75 from the physiological data available in references [Dinnar, 1981; Flaherty et al., 1972]. Of course, the asymptotic form in (15) is not a good approximation to the solution of uni-directional flow in a constant radius tube due to time-periodic pressure gradient for such a large value of α^2 as 37.75. In the present work, however, we do not intend to use the solution of the problem of uni-directional pulsatile flow in a tube as our inlet condition. Instead, we want to use the expression of a specific pulsatile flow which has some essential features of the pulsatile blood flow in arteries. As mentioned earlier, the expression in (13) with $\alpha^2=37.75$ and $\varepsilon=0.2$ has several nice features even though it does not have meaning as an asymptotic solution to the problem of uni-directional pulsatile flow in a constant radius tube. Thus, we have used the velocity field in (13) as the inlet condition in all computations.

4. Orthogonal Grid Generation

In order to solve the problem numerically, we first have to generate a good grid system for the given domain. Our numerical scheme is based on the numerically generated boundary-fitted orthogonal curvilinear coordinate system. In this paper, the method of Oh and Kang [1994] is adopted. Oh and Kang's method is a newly developed numerical scheme for generating an orthogonal grid in a simply-connected 2D domain. Their method is non-iterative and flexible in the adjustment of grid spacing. The grid spacing can be controlled mainly by specification of the boundary correspondence up to on three sides of the boundary.

We generated the orthogonal grid systems for the one-point stenosed vessel as well as the periodically stenosed blood vessel. The results are presented in Fig. 4. The equation for the top side boundary ($\partial\Omega_1$) is given as

$$y=1+0.25[\cos\{\pi(x-1.5)\}-1] \quad 0.75\le x\le 1.5$$
$$y=1 \quad 0\le x<0.75,\ 1.5<x\le 8$$

for the one-point stenosed blood vessel and

$$y=0.8+0.2\cos(\pi x) \quad 0\le x\le 4$$

for the periodically stenosed blood vessel. The grid systems were obtained by specifying the boundary correspondence on three sides as ($x=\xi$, $y=$given function for each geometry) on $\partial\Omega_1$, ($x=0$, $y=\eta$) on $\partial\Omega_2$, and ($x=\xi$, $y=0$) on $\partial\Omega_3$.

RESULTS AND DISCUSSIONS

1. One-point Stenosed Blood Vessel

We have solved the equations for both the stream function and the vorticity for the one-point stenosed solid blood vessel. For the initial condition, it is assumed that there is no flow initially inside the vessel. As already described in Fig. 1, the physical model of the blood vessel is 75% stenosed on the basis of the cross sectional area. The pulsatile flow imposed at the inlet is accelerated in the forward direction for the time interval $0<t<\pi$, but the flow is decelerated for $\pi<t<2\pi$. The acceleration and deceleration are repeated as shown earlier in Fig. 3.

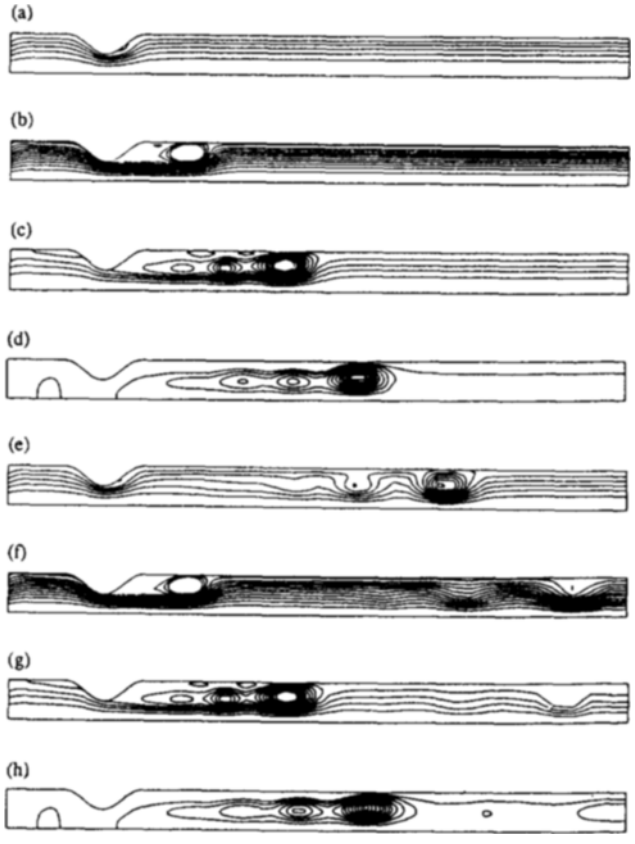

Fig. 5. Streamlines in the one-point stenosed blood vessel for the case of Re=250, St=1.
(a) $t=\pi/2$; (b) $t=\pi$; (c) $t=3\pi/2$; (d) $t=2\pi$; (e) $t=2\pi+\pi/2$; (f) $t=2\pi+\pi$; (g) $t=2\pi+3\pi/2$; (h) $t=4\pi$.

For the case of $Re=250$, $St=1$, the snapshots of streamline distribution inside the blood vessel are shown for several time steps in Fig. 5. At $t=\pi/2$, the vortex seed is formed at the post-stenosed part of the blood vessel. As time goes on, the size of the vortex grows larger and moves downward to the end of the blood vessel. At $t=\pi$, the acceleration phase ends. Although the inlet flow is decelerated after $t=\pi$, the vortex formed during the acceleration period does not disappear and moves to the downstream of the flow. At $t=2\pi$, one period of flow oscillation at the vessel inlet is completed. During the next period, the vortex formed during the first period survives and moves to the downstream. The vortices affect the vessel surface in the form of residual shear stress. The flow fields in the next period near the stenosis are quite similar to those of the previous period.

We have plotted the dimensionless wall vorticity as function of z in Fig. 6. As the dimensionless wall vorticity is directly related to the dimensional shear stress by $\bar{\tau}=-(\mu u_c/l_c)\omega$, we can estimate the shear stress distribution from the vorticity plot along the blood vessel wall. The shear stress oscillates with a large ampli-

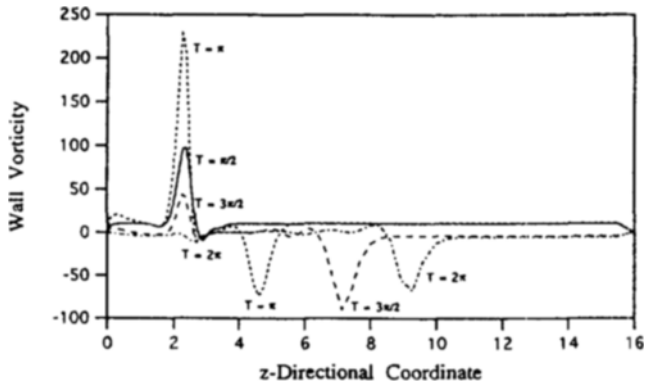

Fig. 6. Distribution of dimensionless vorticity along the wall of the one-point stenosed blood vessel (Re=250, St=1).

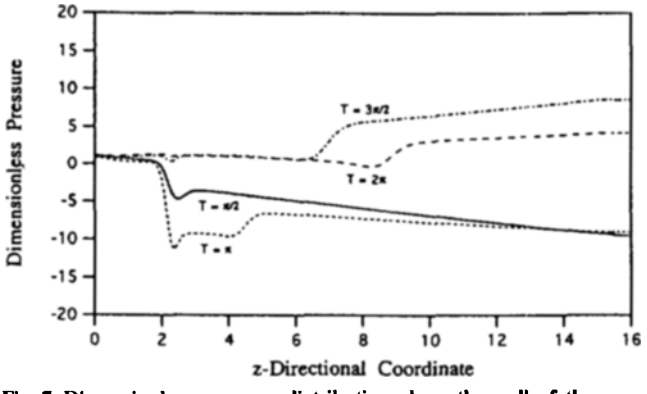

Fig. 7. Dimensionless pressure distribution along the wall of the one-point stenosed blood vessel (Re=250, St=1).

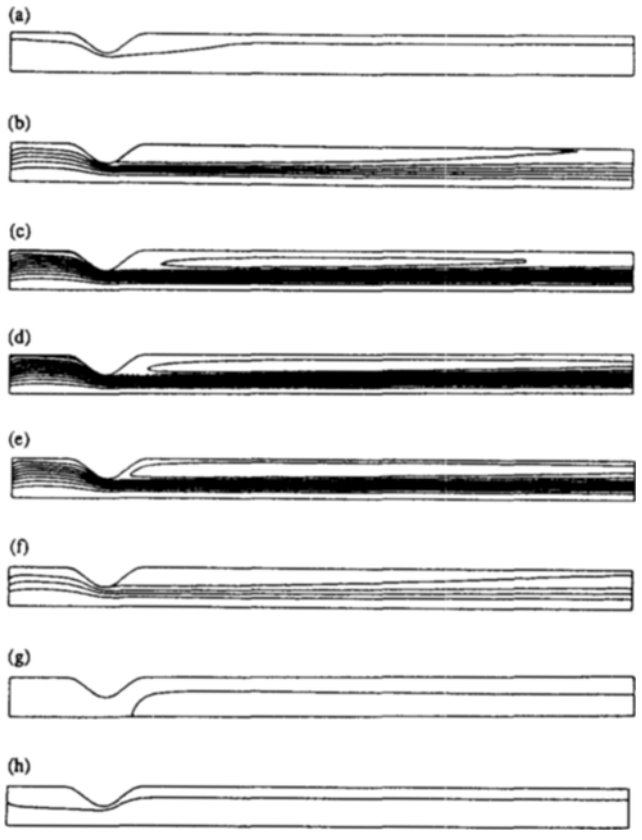

Fig. 8. Streamlines in the one-point stenosed blood vessel for the case of Re=250, St=0.01.
(a) $t=\pi/4$; (b) $t=\pi/2$; (c) $t=3\pi/4$; (d) $t=\pi$; (e) $t=5\pi/4$; (f) $t=3\pi/2$; (g) $t=7\pi/4$; (h) $t=2\pi$.

tude near the stenosis, and there also exists the residual shear stress due to the vortex formed one-period ago. The dimensionless pressure distribution along the vessel is presented in Fig. 7 (The computation of pressure along the wall has been performed by the method in Kang and Leal [1987]). The pressure distribution along the blood vessel wall oscillates as the imposed flow at inlet is accelerated or decelerated.

In the case of Re=250, St=0.01, the flow characteristics are quite different from those of the case of Re=250, St=1 as can be seen from the streamlines in Fig. 8. As mentioned earlier, the Strouhal number is the measure of unsteadiness of the flow field. In the case of Re=250, St=0.01, the flow field at each time step is very similar to that of the steady state flow field that would be obtained when the inlet condition is fixed with the imposed flow at that time. This is due to the small Strouhal number under which the flow field behaves in a quasi-steady state manner. This fact can also be verified from the governing equation (2). Under this condition, a large vortex oscillates in the broad range of the post stenotic region and for the most part of one period there exists a large stagnation flow behind the stenosis. The large stagnation flow has some physiological meaning. The probability of attaching platelets to the surface of blood vessel may be higher in the stagnant region of the blood vessel compared with other vessel segment. If this physiological phenomenon happens, the arterial diseases of stenosis or atherosclerosis become worse and serious damage to the vessel wall may occur. The stenosis will progress further and consequently artificial arterial

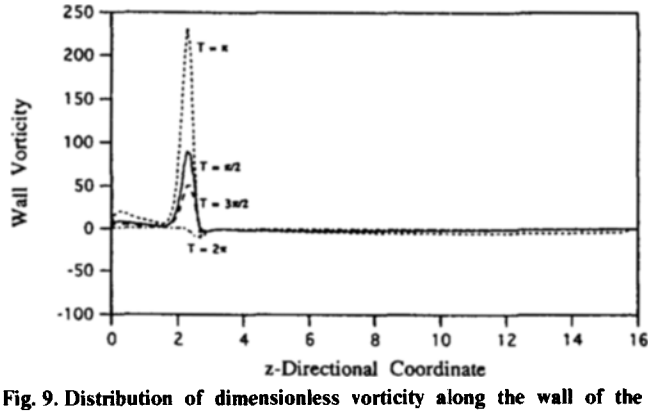

Fig. 9. Distribution of dimensionless vorticity along the wall of the one-point stenosed blood vessel (Re=250, St=0.01).

segment must be prosthesed parallel to the diseased blood vessel [Savvides and Gerrad, 1984].

Fig. 9 shows the distribution of the dimensionless shear stress along the blood vessel wall. Large values of oscillatory shear stress are exerted at the stenosed part of the vessel but there does not exist any residual shear stress far away from the stenotic point of the blood vessel. This is due to the fact that there is no vortex present in that part of the blood vessel. If we look at the pressure variation along the blood vessel shown in Fig.

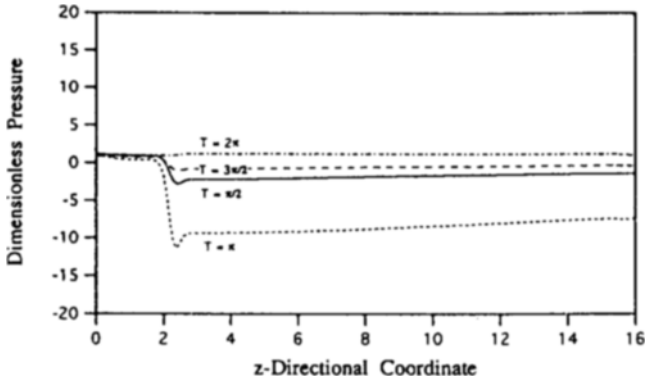

Fig. 10. Dimensionless pressure distribution along the wall of the one-point stenosed blood vessel (Re=250, St=0.01).

Table 2. Numerically calculated shear stress under various flow conditions for each blood vessel type

Model	Shear stress (dyne/cm^2)
Normal blood vessel	23 - − 12 (Re=250, St=1)
One-point	270 - − 105 (Re=250, St=1)
stenosed	270 - − 82 (Re=250, St=0.5)
blood vessel	270 - − 12 (Re=250, St=0.01)
	70 - − 14 (Re=100, St=1)
	70 - − 7 (Re=100, St=0.5)
Periodically	149 - − 67 (Re=250, St=1)
stenosed	146 - − 30 (Re=250, St=0.5)
blood vessel	146 - − 21 (Re=250, St=0.01)
	39 - − 9 (Re=100, St=1)
	39 - − 4 (Re=100, St=0.5)

10, the profiles are nearly the same as that of steady state case at each time. In other words, the profiles show the characteristics of the quasi-steady state.

It is time to investigate the physiological effects of shear stress on the endothelial cells of the blood vessels. As mentioned earlier, the dimensional shear stress ($\tilde{\tau}$) can be computed by using the numerical results of the dimensionless wall vorticity (ω) by the relation $\tilde{\tau} = -(\mu u_c/l_c)\omega$. As an example, we consider a blood vessel of diameter 1 cm (i.e. l_c=radius=0.5 cm) and the viscosity of the blood is assumed to be 3.5 cp (=0.035 g/cm/s). Then from the definition of the Reynolds number u_c is computed. In order to see the effect of the stenosis, the numerical computations have been performed for both the straight blood vessel and the 75% stenosed vessel. For the straight normal blood vessel, the shear stress ranges from 23 dyne/cm^2 to −12 dyne/cm^2 in the case of Re=250, St=1. But for the model of this study, the shear stress value is increased about ten times to the value 270 - − 105 for the same condition and to the 70 - − 14 for the case of Re=100, St=1. At the peak stenosis point the shear stress value oscillates in the range 0-270 dyne/cm^2 for Re=250, St=1, and 0-70 for Re=100, St=1. The numerical values for the other cases are presented in Table 2. This amount of shear stress can cause physical damage to the arterial wall. Daly [1976] suggested that the endothelial surface of the canine thoracic aorta exposed on the time-averaged wall shear stress of 380 dyne/cm^2 (± 85 dyne/cm^2 standard deviation) for approximately 1 hr can be markedly deteriorated. Based on this data we can expect the physical damage of the endothelial surface due to the flow field when there is

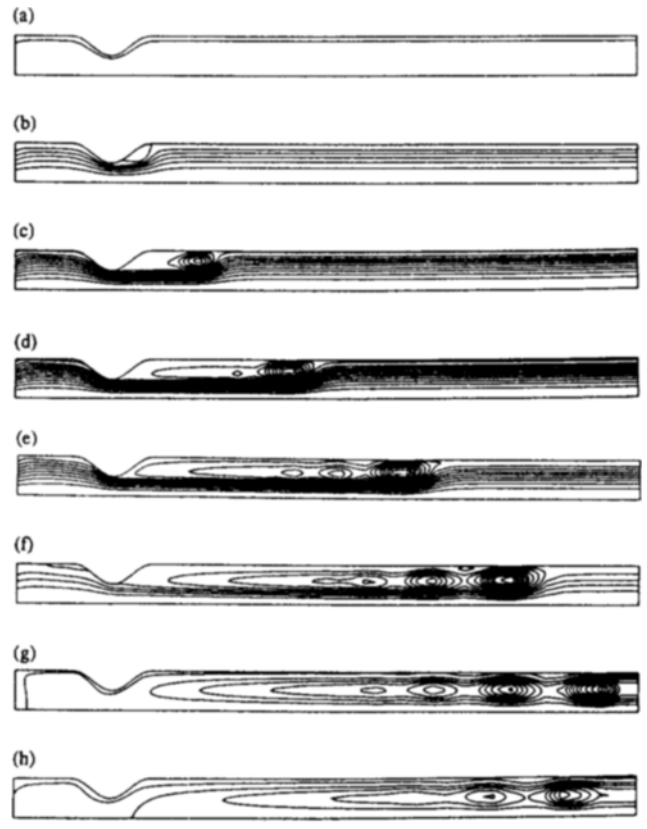

Fig. 11. Streamlines in the one-point stenosed blood vessel for the case of Re=250, St=0.5.
(a) t=π/4; (b) t=π/2; (c) t=3π/4; (d) t=π; (e) t=5π/4; (f) t=3π/2; (g) t=7π/4; (h) t=2π.

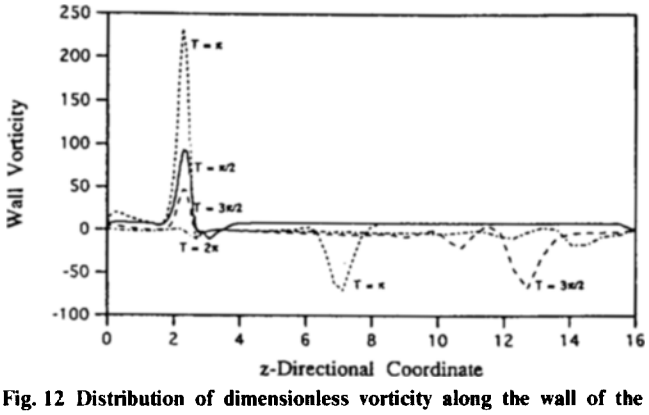

Fig. 12 Distribution of dimensionless vorticity along the wall of the one-point stenosed blood vessel (Re=250, St=0.5).

a deeply developed stenosis.

Now we discuss the effects of the Strouhal number on the flow field characteristics. In the case of a high Strouhal number, unsteadiness of the flow field is prominent. On the other hand, in the low Strouhal number case, the nature of flow field is in a more or less quasi-steady state. The flow with a high Strouhal number of O(1) is dominated by the effect of unsteady acceleration. In this case we have seen from numerical solutions that vortices exist and move to downstream even for a deceleration

phase. The inertial forces cannot erase all the vortices power in the high Strouhal number cases. On the other hand, when the Strouhal number is as small as $O(10^{-2})$, an almost quasi-steady flow exists. Between these orders there is an intermediate Strouhal number at which the flow changes its characteristics from a quasi-steady fashion to a dynamic fashion. In Figs. 11 and 12, the results are shown for the case of $St=0.5$. The results are almost the same as those of the $St=1$ case. Although results are not given in this paper, the numerical solutions for $St=0.1$ case show that the quasi-steady state nature dominates. In the case of $Re=100$, the general behavior is almost the same as that of the $Re=250$ case except that the inertial force is weaker compared with the high Reynolds number case.

2. Periodically Stenosed Blood Vessel

The physical model adopted in this work was given earlier in Fig. 1. The blood vessel is 60% periodically stenosed on the cross-sectional area basis. It is a kind of wavy channel that was adopted by Sobey [1980] or Nishimura [1989]. But the major difference is that our model is rather longer. Sobey considered only one-furrowed channel and Nishimura two-furrowed channel. Our model is a four period furrowed channel. Sobey used the periodic boundary conditions to solve the problem, but in our case, we have solved the problem for the whole system by using the boundary conditions discussed earlier.

For the case of $Re=250$, $St=1$, we have calculated the flow field inside the wavy vessel as a function of time starting from no flow situation. The streamlines at specified times are shown in Fig. 13. As the flow is accelerated, the separation occurs inside the furrowed channel. Initially the flow is subject to a pressure gradient in the direction of the flow because of the acceleration. This causes the fluid to stream through the channel without separation. The channel geometry will impose a pressure gradient opposing the direction of flow in the region of increasing channel width. The magnitude of this adverse pressure gradient will increaseas the flow magnitude increases while the pressure gradient driving the flow will decrease as the time of peak flow is approached. Eventually the adverse pressure gradient will exceed the pressure gradient driving the flow and shortly after this the flow may separate. Once separation occurs, a vortex forms and grows rapidly [Fig. 13(b)] and there may be a considerable region of recirculating flow.

In the deceleration phase, the vortices behave in a remarkable manner. In steady state flow, the vortices decrease in size as the flow magnitude decreases. However, in the case of pulsatile flow, the vortices expand and gradually bulge into the main stream [Fig. 13(c)]. Even though the flux of fluid through the channel vanishes, the vortices remain spinning in the fluid and they effectively occupy the entire channel [Fig. 13(d)]. This behavior is possible because, no matter how the Reynolds number may be large, the continuity of stress of a viscous fluid ensures that moving fluid entrains stationary fluid before the whole fluid would come to rest.

To see the behavior of vortices more closely we took the snapshots with the time interval of $\pi/4$. In Fig. 13(e), we can see that the size of vortex decreases when there is large inertial force that exceeds the vortex power. As the inertial force increases further all the vortices inside the tube are diminished and disappeared completely [Fig. 13(f)]. At the time of $2\pi+3\pi/4$, the new vortices are formed inside the furrow due to the adverse pressure created by geometry [Fig. 13(g)]. As the flow is further accelerated, the vortices grow up and move in the direction of flow inside the furrow. In the deceleration phase of the inlet flow, the vortices grow up in the direction of centerline of the tube. As the flow is more decelerated, the vortices grow further and are about to be ejected to the core of the tube [Fig. 13(j)]. After the vortex

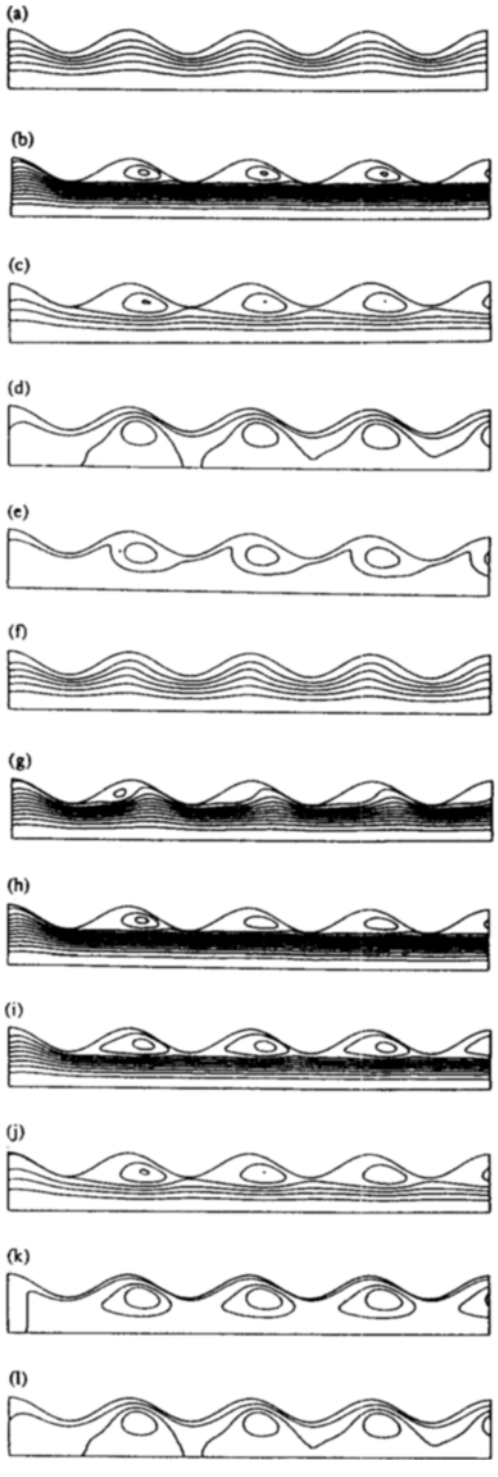

Fig. 13. Streamlines in the periodically stenosed blood vessel for the case of $Re=250$, $St=1$.
(a) $t=\pi/2$; (b) $t=\pi$; (c) $t=3\pi/2$; (d) $t=2\pi$; (e) $t=2\pi+\pi/4\pi$; (f) $t=2\pi+\pi/2$; (g) $t=2\pi+3\pi/4$; (h) $t=2\pi+\pi$; (i) $t=2\pi+5\pi/4$; (j) $t=2\pi+3\pi/2$; (k) $t=2\pi+7\pi/4$; (l) $t=4\pi$.

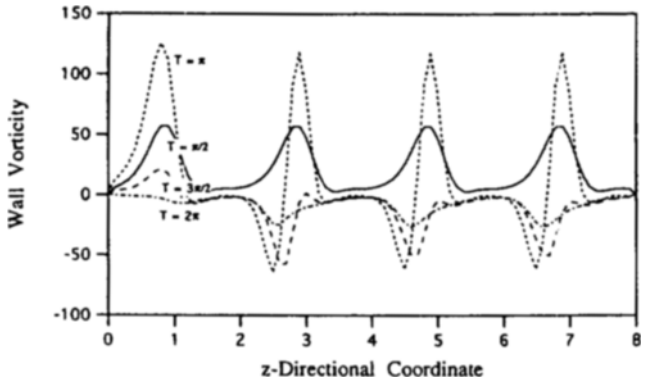

Fig. 14. Distribution of dimensionless vorticity along the wall of the periodically stenosed blood vessel (Re=250, St=1).

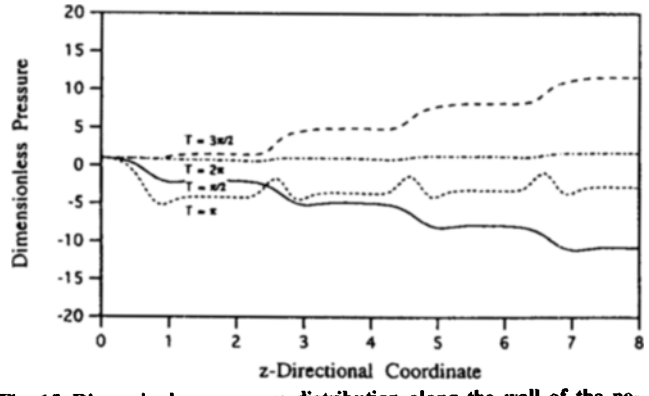

Fig. 15. Dimensionless pressure distribution along the wall of the periodically stenosed blood vessel (Re=250, St=1).

ejection occurs [Fig. 13(k)], the vortex is entrained at the core region between the back flow near the wall surface [Fig. 13(*l*)]. This is the so-called vortex entrainment phenomenon. The process of vortex ejection and entrainment occurs very rapidly at the time of reversal fluid flux.

The process of vortex formation and ejection is a powerful source of convective mixing. A quite striking feature of this flow field is the growth of vortex size during the deceleration period. This phenomenon of existing vortices inside the tube until the inertial force exceeds the vortex power is due to the so-called steady streaming effect. The steady streaming effect is clearly confirmed in our numerical studies. This topic is worthy of further study since some sophisticated equipments for enhancing the heat and mass transport may be designed by taking advantage of the phenomenon mentioned above [Dragon and Grotberg, 1991].

The wall vorticity along the blood vessel is presented in Fig. 14. Large oscillatory shear stresses are exerted to the wall surface near the stenosed point of the blood vessel. In Fig. 15, the pressure variation along the vessel wall is presented. The pressure at the wall changes periodically according to the oscillating flow at the inlet.

For the case of Re=250, St=0.01, the flow fields at various times are presented in Fig. 16, and the wall vorticity along the blood vessel in Fig. 17. As we can see in the figures, the flow fields are nearly the same as the corresponding steady state solutions. Inside the channel, stagnation flow region is formed. Based

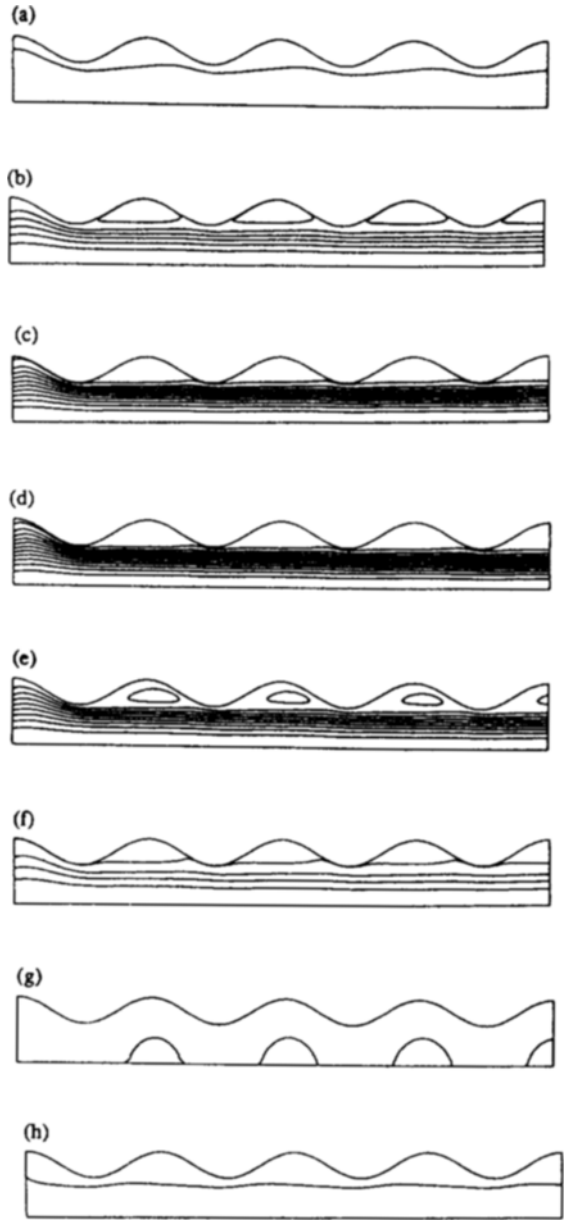

Fig. 16. Streamlines in the periodically stenosed blood vessel for the case of Re=250, St=0.01.
(a) $t=\pi/4$; (b) $t=\pi/2$; (c) $t=3\pi/4$; (d) $t=\pi$; (e) $t=5\pi/4$; (f) $t=3\pi/2$; (g) $t=7\pi/4$; (h) $t=2\pi$.

on these results we can infer that the arterial disease becomes worse once there exists a periodic stenosis along the blood vessel because platelet attachment progresses on the vessel segment between the stenosis points.

Let us now see the increment of shear stress when there is a 64% stenosis compared to that of normal straight arterial segment. As we can see in Table 2, the numerical value of shear stress is increased about 7 times for the 64% periodically formed stenosis. This amount of shear stress may deteriorate the endothelial surface as we can see in Daly [1976].

In the Strouhal number range of $O(10^{-1})$, the flow field shows somewhat intermediate behavior between the dynamic and the quasi-steady states as shown in Figs. 18 and 19. As the Strouhal

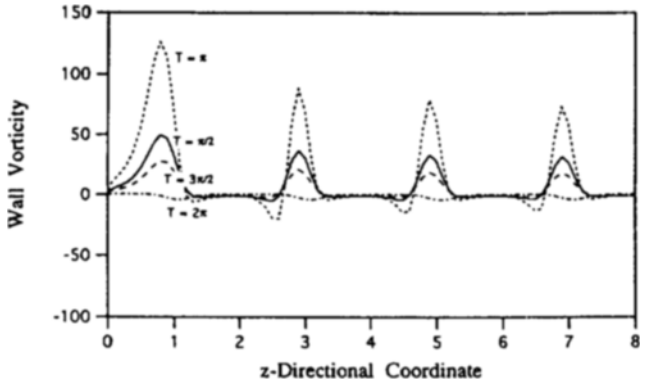

Fig. 17. Distribution of dimensionless vorticity along the wall of the periodically stenosed blood vessel (Re=250, St=0.01).

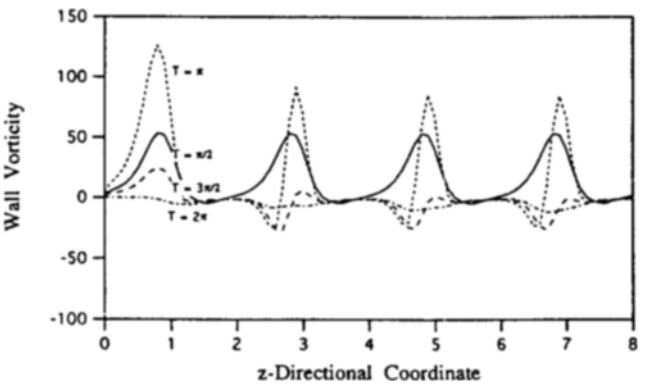

Fig. 19. Distribution of dimensionless vorticity along the wall of the periodically stenosed blood vessel (Re=250, St=0.5).

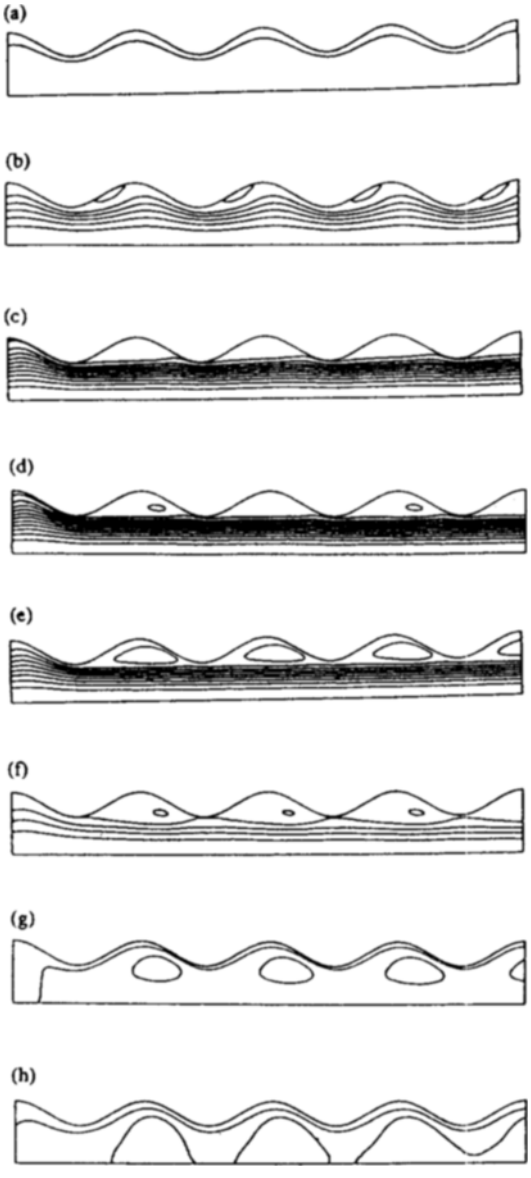

Fig. 18. Streamlines in the periodically stenosed blood vessel for the case of Re=250, St=0.5.

(a) $t=\pi/4$; (b) $t=\pi/2$; (c) $t=3\pi/4$; (d) $t=\pi$; (e) $t=5\pi/4$; (f) $t=3\pi/2$; (g) $t=7\pi/4$; (h) $t=2\pi$.

number is closer to O(1) the unsteady acceleration effect dominates the flow fields, and below the order of $O(10^{-1})$ the flow shows the quasi-steady behavior.

CONCLUSIONS

In this work, several physiological phenomena due to the pulsatile blood flow in fixed but stenosed blood vessels have been studied numerically. The numerical scheme used is the finite difference method with orthogonal grid generation. For convergence scheme of the numerical solutions, ADI scheme has been used. Several important results of the unsteady flow fields inside the blood vessel have been obtained. Based on the results, we expect that the pulsatile blood flow has the following physiological effects in the blood vessel proximal to the stenosis.

- High shear stress is exerted on the blood vessel wall near the stenosed point due to the fast flow, and serious physical damage may occur due to the exerted high shear stress.
- When the Strouhal number is small, there exists a large recirculating flow after the stenosis. The size of the circulating flow oscillates as the imposed flow at the inlet oscillates. The probability of platelet attachment is expected to be higher in the circulating flow region than at other part of the blood vessel.
- When the Strouhal number is O(0.5) or higher, the residual shear stress due to the vortex remained in the post-stenotic region of the blood vessel affects the vessel wall in the form of physical stress.

Another aspect we have confirmed is the steady streaming effect inside the wavy vessel when there is a pulsatile blood flow at the tube inlet. The process of vortex formation→movement →growth→ejection→entrainment is thought to be a powerful source of convective mixing inside the tube without making the flow turbulent. This is an effective way of increasing the heat and mass transfer rate inside the tube. This mechanism may also be applied to enhance the mass transfer rate in some crucial parts of artificial kidney and heart systems.

ACKNOWLEDGMENT

This work was supported by the grant from the Korea Science and Engineering Foundation via the Advanced Fluids Engineering Research Center at the Pohang University of Science and Technology.

REFERENCES

Batchelor, G. K., "An Introduction to Fluid Dynamics", Cambridge University Press, Cambridge, 1967.

Daly, B. J., "A Numerical Study of Pulsatile Flow through Stenosed Canine Femoral Arteries", *J. Biomechanics*, **9**, 465 (1976).

Dinnar, U., "Cardiovascular Fluid Dynamics", CRC Press, Inc. U.S. A., 1981.

Dragon, C. A. and Grotberg, J. B., "Oscillatory Flow and Mass Transport in a Flexible Tube", *J. Fluid Mechanics*, **231**, 135 (1991).

Dutta, A., Wang, D. M. and Tarbell, J. M., "Numerical Analysis of Flow in an Elastic Artery Model", *ASME Journal of Biomechanical Engineering*, **114**, 26 (1992).

Flaherty, J. T., Pierce, J. E., Ferraus, V. J., Patel, D. J., Tucker, W. K. and Fry, D. L., "Endothelial Nuclear Patterns in the Canine Arterial Tree with Particular Reference to Hemodynamic Events", *Circulation Research*, **30**, 23 (1972).

Fung, Y. C., "Biodynamics-Circulation", Springer-Verlag, New York, 1984.

Kaneko, A. and Honji, H., "Double Structures of Steady Streaming in the Oscillatory Viscous Flow over a Wavy Wall", *J. Fluid Mechanics*, **93**, 727 (1979).

Kang, I. S. and Leal, L. G., "Numerical Solution of Axisymmetric, Unsteady Free-Boundary Problems at Finite Reynolds Number. 1. Finite Difference Scheme and Its Application to the Deformation of a Bubble in a Uniaxial Straining Flow", *Phys. Fluids*, **30**, 1929 (1987).

Leal, L. G., "Laminar Flow and Convective Transport Process", Butterworth-Heinemann, Boston, 1992.

Ling, S. C. and Atabek, H. B., "A Nonlinear Analysis of Pulsatile Flow in Arteries", *J. Fluid Mechanics*, **55**, 493 (1972).

Ma, X., Lee, G. C. and Wu, S. G., "Numerical Simulation for the Propagating of Nonlinear Pulsatile Waves in Arteries", *ASME Journal of Biomechanical Engineering*, **114**, 490 (1992).

Nishimura, T., "Oscillatory Viscous Flow in Symmetric Wavy-Walled Channels", *Chemical Engineering Science*, **44**, 2137 (1989).

Oh, H. J. and Kang, I. S., "A Non-Iterative Scheme for Orthogonal Grid Generation with Control Function and Specified Boundary Correspondence on Three Sides", *J. Comput. Phys.*, **112**, 138 (1994).

Patel, D. J. and Vaishnav, R. N., "Basic Hemodynamics and Its Role in Disease Processes", University Park Press, Baltimore, 1980.

Pedley, T. J., "The Fluid Mechanics of Large Blood Vessels", Cambridge University Press., Cambridge, 1980.

Savvides, C. N. and Gerrard, J. H., "Numerical Analysis of the Flow through a Corrugated Tube with Application to Arterial Protheses", *J. Fluid Mechanics*, **138**, 129 (1984).

Sobey, I. J., "On Flow through Furrowed Channels", *J. Fluid Mechanics*, **96**, 1 (1980).

Sobey, I. J., "Oscillatory Flows at Intermediate Strouhal Number in Axisymmetric Channels", *J. Fluid Mechanics*, **134**, 247 (1983).

Tutty, O. R., "Pulsatile Flow in a Constricted Channel", *ASME Journal of Biomechanical Engineering*, **114**, 50 (1992).

Wang, D. M. and Tarbell, J. M., "Nonlinear Analysis of Flow in an Elastic Tube (Artery): Steady Streaming Effects", *J. Fluid Mechanics*, **239**, 341 (1992).

Womersley, J. R., "Method for the Calculation of Velocity, Rate of Flow and Viscous Drag in Arteries When the Pressure Gradient Is Known", *Phil. Mag.*, **46**, 199 (1955).

Wu, S. G., Lee, G. C. and Tseng, N. T., "Nonlinear Elastic Analysis of Blood Vessels", *ASME Journal of Biomechanical Engineering*, **106**, 376 (1984).